# INVESTIGATION OF DIAGONAL CUT–PLANE BPM PERFORMANCE IN THE CSNS RCS*

M. A. Rehman, L. Fang, X. Li, M. Liu, R. Liu, X. Nie, R. Qiu, S. Wang, C. Xie, Z. Xu, R. Yang†
Institute of High Energy Physics, Chinese Academy of Sciences (CAS), Beijing, China
also at Spallation Neutron Source Science Center, Dongguan, China

*Abstract*

Diagonal-cut plane Beam Position Monitors (BPMs) are used to measure the transverse position of the proton beam in the Rapid Cycling Synchrotron (RCS) at the China Spallation Neutron Source (CSNS). Significant transverse beam position offsets were observed at several locations along the RCS. These offsets are potentially attributable to abrupt changes in the cross-section of the upstream and downstream vacuum ducts, BPM calibration constants determined at a single frequency on the calibration system, and limitations in the position calculation algorithm. To assess the impact of the sudden changes in beam duct aperture, numerical simulations were performed. Additionally, BPMs were re-calibrated on a test bench to evaluate the influence of abrupt cross-sectional changes in the BPM and vacuum ducts on the observed offsets at different frequencies.

## INTRODUCTION

The China Spallation Neutron Source (CSNS) [1, 2] is a high-intensity pulsed neutron facility designed to support a broad range of scientific research and industrial applications. Its accelerator system consists of three main components, an 80 MeV $H^-$ beam linac, a 1.6 GeV Rapid Cycling Synchrotron (RCS), and a solid tungsten target station. The 80 MeV $H^-$ beam is injected into the RCS by multi-turn charge-exchange process. The RCS subsequently accelerates the proton beam to 1.6 GeV, achieving a beam intensity of $1.56\times10^{13}$ ppb and a nominal beam power of 100 kW. Recent upgrades, including the installation of harmonic cavities and an improved injection painting scheme, have successfully increased the beam power to 185 kW [3].

The diagonal cut–plane beam position monitor (BPM) has been used in CSNS RCS to accurately measure the transverse beam position of the proton beam during the injection painting and beam energy ramping. During beam studies and routine operation, unphysical transverse position offsets have been observed at several locations along the RCS. It was found that when the beam passes through sections where the beam duct and BPM have different diameters or shapes, the electromagnetic (EM) field of the beam is significantly distorted near the edges of the BPM, this distortion of beam EM field results in unphysical and know as edge effect [4]. A similar issue also has been reported for the in J-PARC MR [5].

* Work supported by the National Science Foundation for Young Scientists of China (12305166).
† yangrenjun@ihep.ac.cn

To investigate and compensate for these unwanted transverse position offsets, four BPMs in the RCS were removed during the 2025 summer maintenance period. The BPMs were re-calibrated using realistic upstream and downstream dummy pipes to accurately incorporate the edge effects into the calibration equations. In addition, CST Wakefield simulations were performed for four different combinations of upstream and downstream beam pipe cross-sections in the BPM region. The wire calibration results and simulation are in good agreement with each other.

## DIAGONAL CUT–PLANE BPM

The 32 diagonal cut–plane BPMs in the RCS are installed to provide transverse position measurements for the injection painting and circulating beam as well for the tune measurement. The diagonal cut–plane BPMs consist of two electrodes separated by a slanted cut, where the induced charge on each plate varies linearly with the beam's transverse position. This design is advantageous for an RCS because it provides a highly linear response over a large region of the vacuum duct's aperture [6, 7]. Given the rapid ramping of magnetic fields and the significant beam excursions during the injection and acceleration phases in an RCS, this linearity ensures accurate beam position measurement. The BPM inner diameter is 220 mm. A 3D schematic view of the RCS diagonal cut–plane BPM is shown in Fig. 1.

Table 1: RCS Diagonal Cut-plane BPM Parameters

| Parameters | Values |
|---|---|
| Inner diameter | 220 mm |
| Electrode Length | 84 mm |
| Material | Ti-6Al-4V |
| Capacitance | 300 pF |
| Electrode Isolation | −40 dB |
| Position Accuracy | 1 % half of Aperture |

Due to the stringent space constraints in the RCS, the BPM must be installed inside the AC corrector magnet. To minimize power dissipation in the BPM body due to eddy currents, a ribbed structure is incorporated on its grounded housing. The BPM is made of Ti-Alloy (Ti-6Al-4V), which has a low electrical conductivity of $5.8 \times 10^5$ S/m, which further suppresses eddy-current heating [8].

Two adjacent electrodes are separated by a 3 mm gap, which provides the required electrode isolation ($S_{21}$). The cross-talk between two adjacent electrodes in the frequency range (1.02–2.44 MHz) is approximately −40 dB. Long alu-

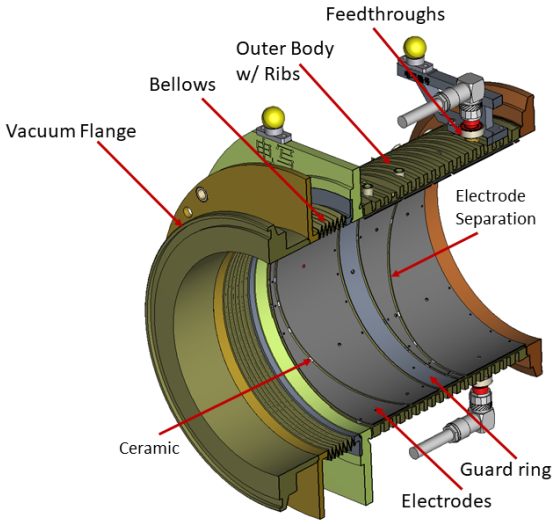


Figure 1: The 3D model of the diagonal cut-plane BPM. The diagonal cut BPM consists of a cylinder that is cut diagonally into two sets electrodes. A grounded guard has been placed between the horizontal and vertical electrodes to prevent coupling between transverse planes.

mina ceramic bars ($Al_2O_3$, 99 %) are placed longitudinally between the electrodes and the grounded body. The relative permittivity of the ceramic is approximately 9.9. The capacitance of each electrode is approximately 300 pF. The position measurement accuracy is 1 % of the half-aperture of the BPM with the resolution of about 200 µm. The parameters of the BPM are listed in Table 1.

## EDGE EFFECT

The edge effect in BPM refers to the distortion of the beam's electromagnetic field caused by geometric discontinuities in the vacuum duct, such as abrupt transitions between different cross-sections, flanges, or bellows located near the BPM. In a perfectly uniform, infinitely long pipe, a relativistic beam is accompanied by a transverse electromagnetic (TEM) field where the image currents perfectly mirror the beam's transverse distribution. However, when the beam passes a change in the vacuum duct geometry, the boundary conditions for the field lines are suddenly changed. This results in image current distribution on the BPM electrodes is no longer purely a function of the beam's position, but also a function of the longitudinal distance from the discontinuity. This results in a shift of the electrical center and a reduction in the effective sensitivity of the BPM. The perturbation charge ($q_P$) induced on a BPM electrode at a distance $g$ from the junction can be given by a first-order approximation [4]

$$q_P(g) \approx \lambda \cdot a \cdot F_{11} \cdot e^{-\frac{\pi g}{a}}, \qquad (1)$$

$\lambda$ represents the line charge density of the beam, while $a$ denotes the half-width of the beam pipe. $R$ is the pipe radius. The variable $g$ signifies the length of the guard ring, which is the longitudinal distance from the pipe junction to the start of the electrode. $F_{11}$ is a dimensionless coefficient determined by the ratio of the joining pipes dimensions.

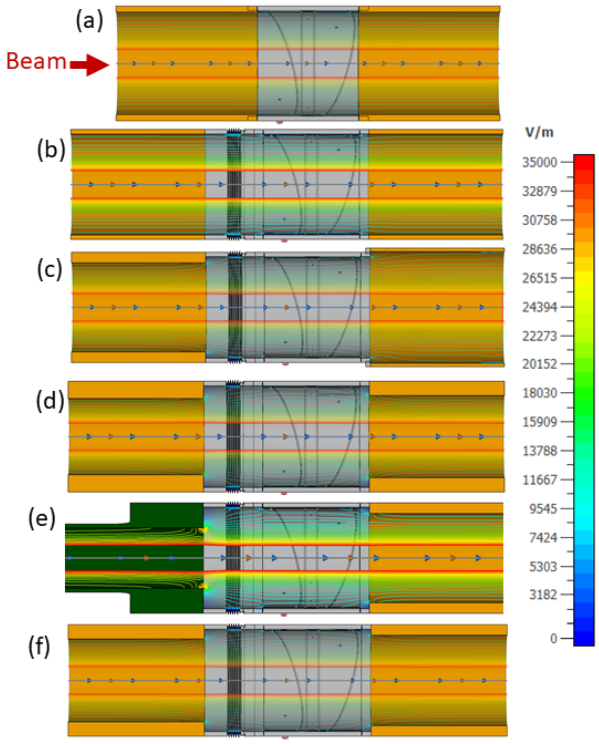


Figure 2: CST simulations of beam electric field lines for six different BPM configurations with upstream and downstream dummy pipes. The distortion of the electric field due to varying dummy pipe cross-sections is clearly visible.

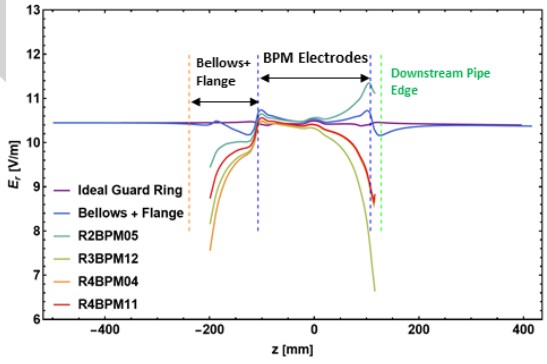


Figure 3: Electric field curves for the different BPM and dummy pipe configurations.

While this analytical formulation provides a fundamental understanding of how edge effects decay, it is primarily applicable to simple, idealized geometries with high degrees of symmetry. In a real-world accelerator environment, BPM installations often involve complex, bellows, and non-uniform apertures that deviate significantly from these basic assumptions. Therefore, for detailed studies numerical simulations [9] have been carried out to accurately account for the fringe fields and determine the precise electrical center.

Figure 2 illustrates CST wakefield simulation of beam electric field lines across six RCS BPM configurations, describing the field distortions induced by varying vacuum

chamber cross-sections. While configuration (a) serves as a reference with a uniform 220 mm diameter, the subsequent cases demonstrate the impact of geometric discontinuities, (b) incorporates bellows and flange-matched diameters, while (c) through (f) replicate specific RCS environments including R2BPM05 (199 mm to 249 mm), R3BPM12 (170 mm to 183 mm), R4BPM11 (183 mm to 200 mm), and the transition from a 135 mm vertical aperture racetrack pipe to a 199 mm circular pipe in R4BPM04.

Figure 3 depicts the induced electric field distribution along the longitudinal axis on the inner surface of the beam duct for various BPM and dummy pipe configurations. A significant distortion of the electric field is observed at the junctions where the cross-sectional geometry changes. These electric profiles highlight how geometric discontinuities at the upstream and downstream interfaces perturb the image current distribution and shifting the electrical center of the beam relative to the physical center of the BPM.

## RE-CALIBRATION OF THE BPM

In order to quantify the impact of edge effect on the BPM the four BPMs were re-calibrated. The BPM calibration was conducted using a stretched-wire system, employing a molybdenum wire with a diameter of 100 $\mu$m. The wire was aligned to the mechanical center of the BPM with an accuracy of 100 $\mu$m. Transverse mapping of the BPM was performed over a range of ±60 mm using a motorized stage with a measured precision of 5 $\mu$m [10]. A signal generator was used to provided a 5 V excitation signal to the stretched wire, typically at a frequency of 0.5-10 MHz. Signal acquisition and processing was done by Bergoz–BB electronics [11], which offer a dynamic range from −70 dBm to +5 dBm and a bandwidth of 10 MHz.

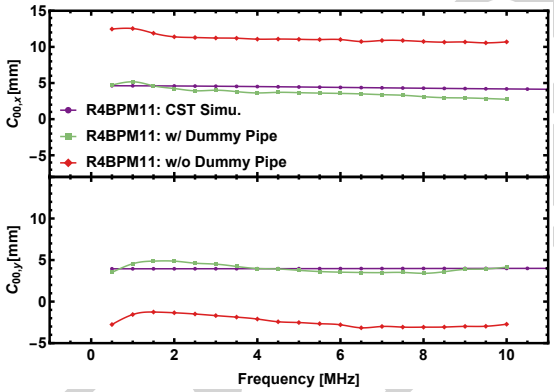


Figure 4: Comparison of the transverse offset of R4BPM11 obtained from BPM re-calibration with and without a realistic dummy pipe, together with the corresponding CST wakefield simulation results.

A third-order polynomial fit was applied to the mapping data to obtain the calibration equations. Figure 4 shows the horizontal and vertical offsets of R4BPM11 as a function of frequency, obtained from CST simulations with realistic cross-sectional transitions, calibration without dummy pipes, and with realistic upstream and downstream dummy pipes. A good agreement is observed between the numerical simulations and the wire calibration results when realistic dummy pipes are used. Similar behavior and agreement were found for the other calibrated BPMs (R2BPM05, R3BPM12, and R4BPM04). The results indicate that the transverse offsets and first order term vary by approximately 5 mm to 7 mm depending on the BPM.

The new calibration equations were implemented for BPM data acquisition. Figure 5 shows the bunch-by-bunch beam position data for R4BPM11. With the updated calibration equation obtained using realistic dummy pipes, the measured transverse position offsets shifted by approximately 3 mm to 5 mm, depending on the specific BPM location.

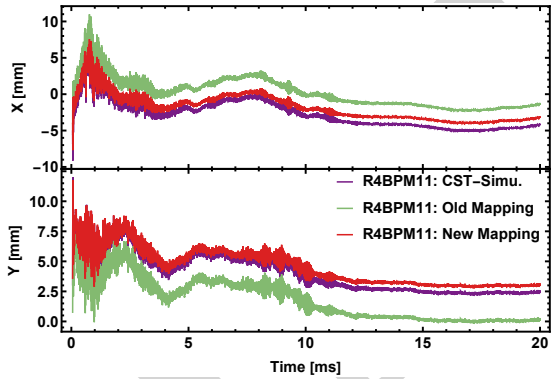


Figure 5: Comparison of bunch-by-bunch transverse beam positions for R4BPM11 using three calibration approaches, the simulated calibration equation, calibration with an ideal dummy pipe, re-calibration with a realistic dummy pipe.

## SUMMARY

The unphysical transverse position offsets observed in the CSNS RCS caused by the edge effect. To investigate this, four diagonal cut-plane BPMs were re-calibrated using a stretched-wire calibration system integrated with realistic dummy pipes that replicated the specific upstream and downstream cross-sections in the RCS. These experimental results were cross-validated with CST Wakefield simulations of various configurations, which reveal the transverse electrical offsets shift by 5 mm to 7 mm and also change the first-order sensitivity terms. By implementing these new calibration equations into the RCS BPM system, the bunch-by-bunch beam position data was corrected by 3 mm to 5 mm.

## ACKNOWLEDGMENTS

We thank Prof. L. Ma (IHEP), Prof. T. Toyama (J-APRC), Prof. K. Satou (J-PARC) and Dr. P. Forck (GSI) for fruitful discussions.

## REFERENCES

[1] J. Wei, *et al.*, "China Spallation Neutron Source: Design, R & D and Outlook", *Nucl. Instrum. Methods Phys. Res. A*, vol. 600, pp. 10–13, 2009. doi:10.1016/j.nima.2008.11.017

[2] W. Sheng, *et al.*, "Introduction to the overall physics design of CSNS accelerators", *Chin. Phys. C*, vol. 33, pp. 1–3, 2009. doi:10.1088/1674-1137/33/S2/001

[3] L. Huang *et al.*, "Intense Beam Issues in CSNS Accelerator Beam Commissioning", in *Proc. HB'23*, Geneva, Switzerland, Oct. 2023, pp. 16–22. doi:10.18429/JACoW-HB2023-MOA1I3

[4] J.H. Cupérus, "Edge effect in beam monitors ", *Nucl. Instrum. Methods Phys. Res. A*, vol. 145, pp. 233–243, 1977. doi:10.1016/0029-554X(77)90415-3

[5] T. Toyama *et al.*, "Performance of the Main Ring BPM during the Beam Commissioning at J-PARC", in *Proc. IPAC'10*, Kyoto, Japan, May 2010, paper MOPE012, pp. 981–983.

[6] Robert E. Shafer. "Beam position monitor sensitivity for low β-beams", *AIP Conf. Proc.* , vol. 319, pp. 303–308, 1994. doi:10.1063/1.46975

[7] P. Forck, P. Kowina, and D. Liakin, "Beam Position Monitors", in *CAS - CERN Accelerator School: Beam Diagnostics*, pp. 187–228, 2009. doi:10.5170/CERN-2009-005.187

[8] M. A. Rehman, *et al.*, "Development of a rectangular diagonal cut-plane BPM for the CSNS-II injection upgrade", *Proc. IBIC'25*, Liverpool, UK, Sep 2025, pp. 645–649. doi:10.18429/JACoW-IBIC2025-WEPC012

[9] CST, https://www.3ds.com/products/simulia/cst-studio-suite

[10] M. A. Rehman, *et al.*, "Development and operation of shorted stripline BPM system for the CSNS LINAC", *Nucl. Instrum. Methods Phys. Res. A*, vol. 1072, p. 170671, 2025. doi:10.1016/j.nima.2025.170671

[11] Bergoz Instrumentation, https://www.bergoz.com